ELSEVIER

Physica D 146 (2000) 328–340

PHYSICA D

www.elsevier.com/locate/physd

# Dual fronts in a phase field model

Karl Glasner [a,*], Robert Almgren [b]

[a] *Department of Mathematics, University of Utah, 155 S. 1400 E., Salt Lake City, UT 84112-0090, USA*
[b] *Department of Mathematics, University of Chicago, 5734 S. University Ave., Chicago, IL 60637, USA*

Received 15 February 1999; received in revised form 17 July 2000; accepted 25 July 2000
Communicated by C.K.R.T. Jones

**Abstract**

We study a dual front behavior observed in a reaction–diffusion system arising initially in the context of phase field models. A precursor front propagates into a stable phase, generating a metastable "intermediate phase". This intermediate phase then decays via an oscillating front, producing a periodic structure which later coarsens. Unlike previously studied models in which dual fronts appear, the appearance of the split front is controlled not by an interchange of wave speeds, but by the existence of the precursor wave. By means of an expansion in small thermal diffusivity, we argue that this behavior is generic.


*Keywords:* Dual front; Intermediate phase; Reaction–diffusion system

## 1. Introduction

An important element in the study of pattern formation is the propagation of fronts by means of which the system moves from one state to another. For example, if the system is initially prepared in a uniform stationary state B (stable or unstable), then we would write B → A to denote a front advancing into the B state, leaving a (presumably stable) state A in its wake. The speed of advance, $v_{AB}$, is determined by the properties of the states A and B, and the dynamics of the system.

In systems possessing three stationary states, A, B, and C, there is a wider variety of possibilities. We shall suppose that the system is initially prepared in state C, and that state A is in some sense the "most stable" state to which the system is attracted. The decomposition from C to A may proceed either by means of a single front C → A with a velocity $v_{AC}$, or via the "intermediate" state B as the pair of fronts C → B → A with velocities $v_{BC}$ and $v_{AB}$ (Fig. 1).

The stability of the phases A, B and C are of great importance in characterizing types of dual front behavior. Bechhoefer et al. [5,27] considered the case

$$\text{stable C} \rightarrow \text{stable B} \rightarrow \text{stable A} \tag{1}$$

* Corresponding author.
*E-mail address:* glasner@math.utah.edu (K. Glasner).

0167-2789/00/$ – see front matter 
PII: S0167-2789(00)00155-X

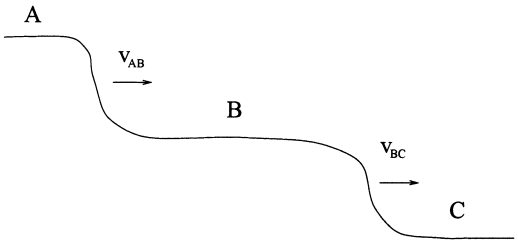


Fig. 1. Schematic view of dual connecting three states. This is sketched as though the state were characterized by a single parameter, though most systems of interest have multiple state components.

as a model of the dynamical generation of the "metastable" state B; although B is stable to small perturbations, it is driven out by A. Both fronts AB and BC in this model are both of "bistable" type: their speeds can be determined by a well-known mechanical analogy (see, e.g., [8]) which gives unique wave speeds.

For this case, [5,27] established that, as system parameters were varied, a necessary and sufficient condition for the appearance of the intermediate state B was that

$$v_{\mathrm{AB}} < v_{\mathrm{BC}}. \tag{2}$$

If (2) is satisfied, then the system generates a longer and longer stretch of state B as the fronts advance; conversely, if it is violated, then the trailing front will always catch up to the precursor front and coalesce with it. (Csahok and Misbah [9] have considered a situation where the trailing front is repelled by the leading one, and the dual front structure remains intact, but we may consider this structure as a single compound front.) Fife and McLeod [12] showed rigorously for a single-component system that (2) was indeed necessary and sufficient for the appearance of dual fronts.

Elmer et al. [11] considered a two-component system with

$$\text{unstable C} \rightarrow \text{unstable B} \rightarrow \text{stable A} \tag{3}$$

in which state B has a saddle point structure. The precursor wave BC enters state B along its stable manifold and this state decomposes along its unstable manifold, ending in state A. In this case, both waves are of "monostable" type, and their speeds may be determined by the heuristic theory of marginal stability [10,30] which essentially states that it is the linearized behavior near the unstable state which determines the front speed (for many systems, marginal stability gives the correct speed, and the extended notion of "nonlinear marginal stability" [31] is not necessary). Elmer et al. concluded that again, condition (2) was necessary and sufficient for the appearance of two fronts. The existence of dual fronts in this case is rather remarkable, since the system is generating an increasingly large amount of *unstable* state as the fronts advance. Dual fronts of this type also appear in amplitude equations for competition between roll and hexagonal convection patterns [9,24].

We are interested in a system whose structure is intermediate between (1) and (3). In the language of reaction–diffusion models [17], one of our state variables is "conserved" rather than "nonconserved" as are the variables in the examples above: the spatial integral of this variable is strictly constant, and it can change only by *transport* of the physical quantity it represents. Our intermediate state will be *stable* as a solution of the ordinary differential equation (ODE) which neglects transport, but *unstable* in the dynamics of the full space-dependent problem; we will call it *metastable*.

Our model is the one introduced as Model C by Halperin et al. [17]. These models describe the evolution of two scalar variables: a nonconserved order parameter $\phi(x,t)$ and a conserved "energy" $e(x,t)$ which is constructed from $\phi$ and a "temperature" $u(x,t)$. We shall refer to $e$ as an energy and $u$ as a temperature, which are appropriate

for solidification of a pure material. In different problems these may represent different quantities, e.g., in alloy solidification problems, $e$ may be solute concentration and $u$ may be chemical potential. The variables are scaled so that $u = 0$ represents the coexistence condition between the two phases; if the initial conditions have $u \neq 0$ and $\phi$ representing some phase interface, then fronts will propagate through the domain as the material changes phase. These models have been used successfully for solidification problems [15,20] and have shown agreement with other theories of phase dynamics [6,19,26].

The coupling between the order parameter and the temperature field is controlled by a parameter $\lambda > 0$. For small $\lambda$, the only stable states are bulk liquid and solid, which we shall arbitrarily denote by $\phi = -1, 1$, respectively. Then, typical solutions to the system are propagating fronts joining these two phases. With boundary conditions corresponding to undercooling below freezing temperature, these are solidification fronts. They propagate into the locally stable liquid phase, converting it to the entropically more favorable stable solid phase.

As $\lambda$ is increased, an intermediate state $\phi_{\mathrm{m}}$ appears, metastable as described above, generated by a "precursor" front propagating into the solid phase. The $\phi_{\mathrm{m}}$ phase then destabilizes by a process similar to spinodal decomposition, decaying into a mixture of solid and liquid phases. This behavior was observed independently in [1] and by Zukerman et al. [34]; in those simulations, the destabilization front advances more slowly than the precursor front, and ever-increasing amounts of the intermediate state are generated as time advances.

Clearly, the speed condition (2) is necessary for the appearance of the intermediate phase. It would be natural to suppose that, as for the systems with nonconserved parameters, that production of the intermediate state would be controlled by that condition. Surprisingly, that is not the case.

The new contributions of this paper are as follows:

1. We clarify the role of the intermediate state in the context of thermodynamically consistent models, providing necessary conditions for the dual front's appearance. We show that for fixed (bulk) internal energy, this state is a local minimum of the negative entropy, but nevertheless is destabilized by heat redistribution.
2. We derive the front velocities by an asymptotic analysis of the travelling wave problem for the leading front, and of the marginal stability criteria for the oscillatory instability.
3. We determine that condition (2) is always the case for our situation, if the two fronts exist at all. The crucial aspect of dual front formation here is the existence of the leading wave; even though the intermediate state has lower negative entropy that the initial state, it may be dynamically inaccessible to the time-dependent system. This phenomenon is very different from systems previously studied.
4. We provide a discussion of the physical interpretation of this phenomenon, suggesting links to other phase field theories.

The rest of this paper is as follows. In Section 2, we present our phase-field model, and discuss the appearance of the intermediate state. In Section 3, we determine the propagation velocities of the two fronts numerically. In Section 4, we carry out an asymptotic analysis for the two fronts.

## 2. The phase field model and front splitting

We shall work with the model in the "thermodynamically consistent" form [23,32], in one space dimension. In this formulation, we begin with an expression for the total negative entropy of the system

$$S[\phi, e] = \int_{-\infty}^{\infty} \left( s(\phi, e) + \frac{1}{2}\epsilon^2 \phi_x^2 \right) \mathrm{d}x, \tag{4}$$

in which the scalar function $s(\phi, e)$ is the specific negative entropy, and the parameter $\epsilon$ is a length scale which will characterize typical transition layers. The internal energy density $e(x, t)$ is related to the temperature $u(x, t)$

by

$$e = u - \tfrac{1}{2}p(\phi),$$

where $p(\phi)$ with $p(\pm 1) = \pm 1$ is the enthalpy function. Since internal energy is a conserved quantity, it is more convenient to construct the dynamics in terms of $e$ rather than $u$.

We take the specific form

$$s(\phi, e) = g(\phi) + \tfrac{1}{2}\lambda u^2 = g(\phi) + \tfrac{1}{2}\lambda(e + \tfrac{1}{2}p(\phi))^2,$$

where $g(\phi)$ is a smooth double-well potential with minima $g(-1) = g(1)$ and $g'(\pm 1) = 0$. The parameter $\lambda$ simply represents the coupling between the two fields; in the sharp interface limit $\epsilon \to 0$, this parameter may be associated with the inverse surface tension [6]. We require that $p'(\pm 1) = 0$ so that $\phi = \pm 1$ are stationary points of $s$ for any value of $e$, and that $p''(\pm 1) = 0$ so that these stationary points are always local *minima* of $s$. The simplest smooth functions satisfying these conditions are

$$g(\phi) = \tfrac{1}{4}(1 - \phi^2)^2, \qquad p(\phi) = \tfrac{15}{8}\left(\phi - \tfrac{2}{3}\phi^3 + \tfrac{1}{5}\phi^5\right).$$

Our results do not depend on the precise form of $s(\phi, e)$, $g(\phi)$, or $p(\phi)$.

We define the time evolution of $\phi$ and $e$ as a gradient flow for the negative entropy functional $S[\phi, e]$, thereby guaranteeing that $S$ decreases monotonically in time. Corresponding to the interpretation of $\phi$ as a nonconserved quantity, and the integral of $e$ as a conserved quantity, we compute the gradients in the $L^2$ norm for $\phi$ and in the $H^{-1}$ norm for $e$ (see [23,28]).

This yields the evolution equations (see [23,32] for other derivations)

$$\phi_t = -D_\phi \left.\frac{\delta S}{\delta \phi}\right|_{L^2} = D_\phi(f(\phi, u) + \epsilon^2\phi_{xx}), \qquad e_t = -D_u \left.\frac{\delta S}{\delta e}\right|_{H^{-1}} = D_u\lambda\partial_{xx}\left(e + \frac{1}{2}p(\phi)\right) = D_u\lambda u_{xx},$$

in which

$$f(\phi, u) = -\left.\frac{\partial s}{\partial \phi}\right|_e = -g'(\phi) - \frac{1}{2}\lambda u p'(\phi).$$

The constants $D_\phi$, $D_u$ are the rates of relaxation for each field. We may nondimensionalize by setting

$$t' = D_\phi t, \qquad x' = \epsilon^{-1}x.$$

After dropping primes, the resulting system has the form

$$\phi_t = f(\phi, u) + \phi_{xx}, \tag{5}$$

$$e_t = Du_{xx}, \tag{6}$$

in which $D = \lambda D_u / D_\phi$ is a nondimensional ratio of thermal diffusivity to phase diffusivity. We note that $D$ is frequently small since phase kinetics are typically much faster than thermal (or material) diffusion.

We are interested in problems where a solidification front is propagating into a uniform supercooled liquid, defined by the boundary conditions

$$\phi(+\infty, t) = -1, \qquad u(+\infty, t) = -\Delta,$$

where $\Delta$ is the nondimensional undercooling. The internal energy in the right state is therefore

$$e(+\infty, t) \equiv e_\infty = \tfrac{1}{2} - \Delta.$$

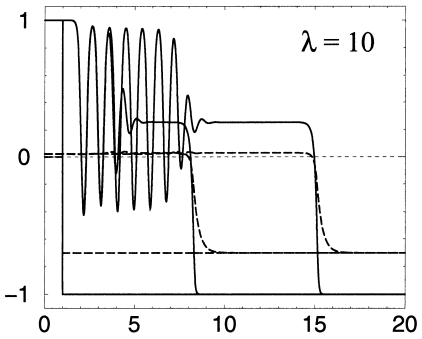


Fig. 2. Time-dependent simulation showing generation of the intermediate state, where the solid curves are $\phi$ and the dotted curves are $u$. The initial condition is the step function on the far left. The other two profiles are for $t = 5$ and 10. The parameters are $\Delta = 0.7$, and $\lambda = 10$ and $D = 1$.

For $\Delta > 0$, the solid state $\phi = 1$ is more favorable than the liquid state $\phi = -1$, and we expect the solution dynamics to be a wave moving to the right, generating solid state with

$$\phi(-\infty, t) = 1.$$

The value of $u$ in the left state is determined by conservation of energy; in a traveling wave solution both end states must have the common value $e = e_\infty$. Thus, a steady wave must have

$$u(-\infty, t) = 1 - \Delta \quad \text{so that } e(-\infty, t) = e_\infty.$$

If $\Delta < 1$, then the solid generated is superheated with $u > 0$. If $\Delta$ is too far from 1, then constant-velocity waves are impossible; near $\Delta = 1$, the wave speeds have a rich and interesting structure [16,21,22].

However, as noted independently by Almgren and Almgren [1] in one-dimensional simulations, and by Zukerman et al. [34] for two-dimensional simulations, such a smooth front is commonly *not* what is observed in simulations. Fig. 2 shows a time-dependent simulation which attempts to model a freezing interface with $\Delta = 0.7$. The expected wave front joining liquid with $\phi = -1$ to solid with $\phi = 1$ has decomposed into a pair of fronts. The first front joins the liquid state to a spatially uniform state in which the phase and temperature have intermediate values $\phi = \phi_\mathrm{m}$ and $u = u_\mathrm{m}$. This intermediate state is then unstable to an oscillatory perturbation, whose envelope follows the first wave front. We shall describe reasons for this situation to exist.

To develop some intuition, we will first consider two simplified cases: first, the ODE describing the dynamics of spatially uniform states, obtained by suppressing spatial dependence on the right-hand sides of (5) and (6); and second, the single ODE obtained by setting $D = 0$ in (6).

### 2.1. Ordinary differential equation

Suppressing spatial derivatives in (5) and (6) gives the single ODE

$$\phi_t = -\frac{\partial}{\partial \phi} s(\phi, e),$$

in which $e$ rather than $u$ is held constant as $\phi$ varies. Stable stationary points correspond to local minima of $s(\phi, e)$ over $\phi$ for a given value of $e$. These minima are illustrated in Fig. 3.

For large $\lambda$, an internal local minimum of $s$ can exist. We make the following definition.

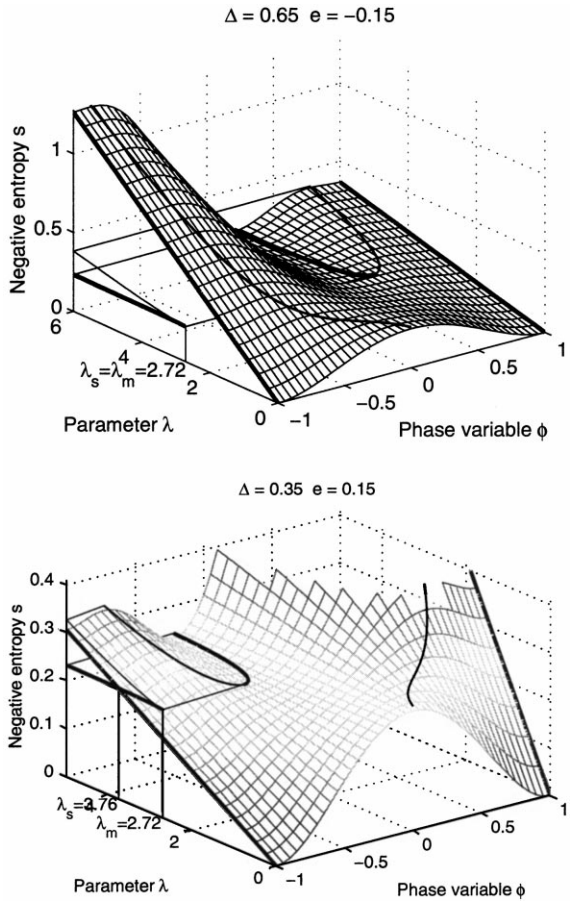


Fig. 3. Plots of $s(\phi, e; \lambda)$ for two different values of $e$. Lines show local minima of $s$ over $\phi$; light lines are local maxima. Graph (a) has $\Delta = 0.65$ and $e = -0.15$; the intermediate minimum has, from the beginning of its existence, a *lower* value of $s$ than the liquid state, so that $\lambda_s = \lambda_m$. Graph (b) has $\Delta = 0.35$ and $e = 0.15$; the intermediate minimum initially has a *larger* value of $s$ than the liquid state, so $\lambda_s > \lambda_m$.

**Definition 1.** The first critical parameter value $\lambda_m(e)$ is the smallest value of $\lambda$ above which $s(\phi, e; \lambda)$ has a local minimum in the interval $\phi \in (-1, 1)$. For $\lambda \geq \lambda_m(e)$, the intermediate phase $\phi_m(\lambda, e)$ is the corresponding minimum location.

The dynamics of the ODE are clear: the state $\phi$ flows smoothly downwards to one of its wells. For $\lambda \leq \lambda_m$ there are two such wells at $\phi = \pm 1$; for $\lambda > \lambda_m$ there is an additional third well at $\phi_m$ with $-1 < \phi_m < 1$. If spatially inhomogeneous initial data $\phi_0(x)$ is given (we imagine $e_0(x) \equiv e_0$ is constant), then the solution $\phi(x, t)$ will tend to a steady state in which $\phi$ is piecewise constant at different local wells corresponding to the different basins of attraction of the initial data.

### 2.2. Scalar equation with $D = 0$

If we set $D = 0$, then the dynamics of $\phi(x, t)$ are given by the single scalar equation

$$\phi_t = -\frac{\partial}{\partial \phi} s(\phi, e) + \phi_{xx}, \tag{7}$$

where we suppose that $e(x) \equiv e_0$ is constant. This equation is the well-known Allen–Cahn equation in materials science, and arises in many other contexts.

Spatially uniform states which were stable under the ODE dynamics — $\phi = \pm 1$ and $\phi = \phi_m$ if $\lambda \geq \lambda_m$ — are again stable under this PDE dynamics. If the initial data contains different regions in which $\phi$ is in different stable wells, then fronts will develop in which $\phi$ moves from one well to a deeper well, and the speed of fronts roughly scales as the difference in depth of the wells [25].

Because the overall negative entropy $S[\phi, e]$ is nonincreasing, steady state traveling waves which generate the intermediate state, as illustrated in Fig. 2 can exist only if the intermediate state has a lower value of $s$ than the initial liquid state. We thus define the following definition.

**Definition 2.** The second critical parameter value $\lambda_s(e)$ is the smallest value of $\lambda$ above which the internal minimum $\phi_m$ exists, and $s(\phi_m, e; \lambda) \leq s(-1, e_\infty; \lambda)$. (This may be the same value as $\lambda_m$ defined above.)

For small values of $e$, corresponding to high undercoolings, the intermediate state can satisfy this condition from the beginning of its existence at $\lambda = \lambda_m$. In this case we take $\lambda_s = \lambda_m$. Note that the local behavior of $s$ near $\phi_m$ at $\lambda = \lambda_s$ is different depending on whether $\lambda_s = \lambda_m$ or $\lambda_s > \lambda_m$.

With $D = 0$, the intermediate state $\phi_m$ is stable under the dynamics (7); thus increasing amounts of intermediate state are generated as time evolves. The effect of introducing $D > 0$ is to *destabilize* the intermediate state, yielding the oscillating trailing front in Fig. 2. In previous studies of dual front dynamics, the presence of the dual front structure depended on the relative speeds of the leading and the trailing fronts. The purpose of this paper is to analyze the effects of $D \neq 0$ and especially to carry out an asymptotic analysis for $D$ near zero, and argue that the speed ordering does not determine the presence or absence of dual fronts.

As a final note, let us point out that both critical values of $\lambda$ necessarily exist for any continuous constitutive functions $g(\phi)$ and $p(\phi)$ as long as $0 < \Delta < 1$ so that $|e| < \frac{1}{2}$. To see this, note that under this condition and for continuous $p(\phi)$ with $p(\pm 1) = \pm 1$, the quantity $(e + \frac{1}{2}p(\phi))^2$ necessarily has at least one zero for $-1 < \phi < 1$, and takes finite values at the endpoints that are at least as large as $(\frac{1}{2} - |e|)^2$. A sufficient condition for $s(\phi, e)$ to have an internal minimum at which $s$ is smaller than at $\phi = -1$ is then that $\frac{1}{2}\lambda(\frac{1}{2} - |e|)^2 \geq \max_{|\phi|\leq 1} g(\phi)$, which is always true when $\lambda$ is large enough. Thus, the behavior shown in Fig. 3 is generic.

## 3. Propagation velocities

We will now consider what happens in general with $D \neq 0$. What distinguishes our dual front scenario from others which have been studied is that the two front speeds are determined by entirely different mechanisms. The leading front's speed is determined by solving a nonlinear eigenvalue problem, whereas the oscillating front's advancement will be given by the linear behavior around the intermediate state. Here, we describe methods which allow us to compute the front velocities.

### 3.1. The oscillating front

The growth rates $\omega(k)$ of perturbations with structure $\exp(\mathrm{i}kx + \omega t)$ to the intermediate state $(\phi_m, u_m)$ are determined as roots of the dispersion relation

$$\omega^2 + [(D+1)k^2 + \sigma]\omega + Dk^2(k^2 - \rho) = 0, \tag{8}$$

where

$$\sigma = -\left( \left.\frac{\partial f}{\partial \phi}\right|_u + \frac{1}{2}p'(\phi) \left.\frac{\partial f}{\partial u}\right|_\phi \right) = \left.\frac{\partial^2 s}{\partial \phi^2}\right|_e, \qquad \rho = \left.\frac{\partial f}{\partial \phi}\right|_u = -\sigma + \frac{1}{4}\lambda p'(\phi)^2,$$

evaluated at $\phi = \phi_m$, $u = u_m$. Notice that $\sigma \geq 0$ for all $\lambda \geq \lambda_m$, and $\sigma \searrow 0$ as $\lambda \searrow \lambda_m$. Solving for $\omega$, we find that there is an unstable band of wavenumbers $0 < k < \sqrt{\rho}$. We will assume that $\rho > 0$; otherwise the intermediate state would be stable, and no oscillatory front would exist. Clearly, $\rho > 0$ near $\lambda = \lambda_m$ as long as $p'(\phi) \neq 0$, and it is easy to check that $\rho > 0$ for the specific polynomial model given in Section 2.

The speed of the advancing instability may be sought using the method of marginal stability [10,30,31]. The velocity $V$ of any perturbation is related to the growth rate and wavenumber by

$$V = \frac{\operatorname{Re}\omega}{\operatorname{Im} k}.$$

The selected velocity and wavenumber must satisfy

$$\frac{\mathrm{d}V}{\mathrm{d}\operatorname{Re} k} = \frac{1}{\operatorname{Im} k}\frac{\mathrm{d}\operatorname{Re}\omega}{\mathrm{d}\operatorname{Re} k} = 0, \tag{9}$$

$$\frac{\operatorname{Re}\omega}{\operatorname{Im} k} = \frac{\mathrm{d}\operatorname{Re}\omega}{\mathrm{d}\operatorname{Im} k}. \tag{10}$$

We have found $V$ by numerically solving (9) and (10) for the marginally stable wavenumber $k = k^*$. Zukerman et al. [34] also computed the marginal stability velocities and found them in accord with time-dependent simulations. As a result, we have reason to believe the validity of this method.

### 3.2. The leading front

If we look for constant velocity traveling wave solutions of the form $\phi = \phi(x - Vt)$, $u = u(x - Vt)$, we obtain the problem

$$\phi'' + V\phi' + f(\phi, u) = 0, \tag{11}$$

$$Du' + Vu - \tfrac{1}{2}Vp(\phi) - Ve_\infty = 0, \tag{12}$$

$$u(+\infty) = -\Delta, \qquad u(-\infty) = u_m, \qquad \phi(+\infty) = -1, \qquad \phi(-\infty) = \phi_m, \tag{13}$$

where $e_\infty = -\Delta + \frac{1}{2}$ is the common value of the internal energy in the stationary states connected by the front. A detailed analysis has been conducted for this problem in [16]. In particular, it was shown that for solutions to exist, $\lambda$ must necessarily be larger than $\lambda_s$, as we have assumed. An asymptotic solution will be carried out later, but for now, we simply describe a method of solving this problem numerically.

As shown in [1], this system has for $V > 0$, a one-dimensional unstable manifold passing through the intermediate state. This forms the basis for a shooting method, since a trajectory on this manifold necessarily satisfies the left hand boundary conditions. To ensure the other boundary condition is satisfied as the trajectory is evolved forward, the parameter $V$ must be adjusted. This was done numerically, and it was found that sometimes exactly two solutions existed, and sometimes none. The results are discussed in the next section.

### 3.3. Numerical results

Fig. 4 shows a typical plot of velocities as a function of $\lambda$ for $\Delta = 0.7$, $e = -0.2$, and compares them to the marginal stability velocities of the oscillatory front. No leading front solutions exist at all below a certain value of $\lambda$; this is typical in all parameter ranges. At a certain point, a saddle-node bifurcation gives rise to two branches of leading front solutions. We have compared these solutions to simulations of the full equations, and it appears that the fast solution branch is the dynamically stable one.

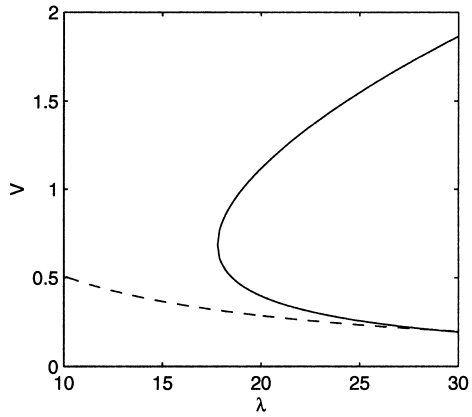


Fig. 4. Velocities of the oscillating front (dashed) and the two branches of the precursor front velocity (solid), for $\Delta = 0.7$ and $D = 4$. The picture is qualitatively the same for other parameters.

For general parameter values, we have found that the leading front is always faster than the oscillating front. Although this ordering of speeds is presently an open question from a rigorous standpoint, we will show that this behavior is generic in the limit of small $D$.

## 4. The small-$D$ limit

Recall from Section 1 that a physically interesting limit is $D \to 0$, corresponding to fast phase kinetics. We shall study the velocities of the leading and oscillatory fronts by means of asymptotic expansions near $D = 0$ and discuss the results.

### *4.1. Oscillating front velocity*

For small values of $D$, the positive growth rate $\omega_+$ solving the dispersion relation (8) has the form

$$\omega_+ = Dk^2 \frac{\rho - k^2}{k^2 + \sigma} + \mathcal{O}(D^2). \tag{14}$$

The leading order solution to (9) and (10), $k^*$, is therefore independent of $D$. As a result, the marginal stability velocity will be of the form

$$V = DV_0(\rho, \sigma) + \mathcal{O}(D^2). \tag{15}$$

An interesting special case is where $\sigma$ is small, e.g., when $\lambda$ is close to $\lambda_s$. Neglecting $\sigma$ in (14), we can solve (9) and (10) exactly, giving the marginal stability velocity

$$V = 2D\sqrt{\rho}. \tag{16}$$

This is the well-known result of Kolmogorov et al. [2,18] for one component systems. Since the growth rate $\omega_+$ is a decreasing function of $\sigma$, (16) should in general provide an upper bound on the velocity when $D$ is small. Note that $\rho$ does not tend to zero as $\lambda \to \lambda_s$. The result that $V \sim \mathcal{O}(D)$ as $D \to 0$ depends only on the local structure of $s(\phi, e)$ near $\phi = \phi_m$, not on the relative values of $s(\phi_m)$ and $s(-1)$.

### 4.2. Leading front velocity

The asymptotic analysis for the problem (11)–(13) will consider two separate cases

1. $s(\phi_{\mathrm{m}})$ *not near* $s(-1)$. This case always applies to the upper branch of solutions (see Fig. 4) far away from the bifurcation point. It also applies near the bifurcation point, as long as $\lambda_s = \lambda_{\mathrm{m}}$ (Fig. 3(a)). In this case, $V$ has a finite limit as $D \to 0$.
2. $s(\phi_{\mathrm{m}})$ *close to* $s(-1)$. This case applies near the bifurcation point $\lambda = \lambda_s$, when $\lambda_s > \lambda_{\mathrm{m}}$. In this case, we make a special asymptotic expansion in $D$ and $\lambda$ simultaneously to show that $V \sim \mathcal{O}(D^{1/2})$.

In both cases, the speed of the precursor front is larger than the speed of the oscillatory front for small $D$.

In Case 1, we assume regular expansions of the form

$$V \sim V_0 + DV_1 + \cdots, \qquad \phi \sim \phi_0 + D\phi_1 + \cdots, \qquad u \sim u_0 + Du_1 + \cdots \quad \text{as } D \to 0.$$

The leading order solution for $u$ then satisfies

$$u_0 - \tfrac{1}{2} p(\phi_0) - e_\infty = 0, \tag{17}$$

and therefore $\phi_0$ is the solution to

$$(\phi_0)'' + V_0(\phi_0)' - s_\phi(\phi_0, e_\infty) = 0. \tag{18}$$

Solutions $(V_0, \phi_0)$ to Eq. (18) exist and are unique up to translation (see, e.g., [13]). Multiplying by $\phi_0'$ and integrating gives

$$V_0 \int_{-\infty}^{\infty} (\phi_0')^2 \, \mathrm{d}x = s(-1, e_\infty) - s(\phi_{\mathrm{m}}, e_\infty).$$

The left-hand side of this expression is positive and $\mathcal{O}(1)$ as long as $\lambda \gg \lambda_s$, and an upper bound on the integral of $(\phi_0')^2$ can be provided (see [16]). Thus, $V_0$ is bounded away from zero and the total velocity satisfies

$$V = V_0 + \mathcal{O}(D). \tag{19}$$

If $\lambda_s > \lambda_{\mathrm{m}}$, then $s(-1, e_\infty) - s(\phi_{\mathrm{m}}, e_\infty)$ is small when $\lambda$ is near $\lambda_s$. In this case, $V_0$ would not be $\mathcal{O}(1)$, and therefore the assumed form of the above asymptotic expansion is incorrect. We rectify this by introducing a different scaling for Case 2.

For $\lambda$ near $\lambda_s$, we introduce the rescaled variable

$$\Lambda = D^{-1/2}(\lambda - \lambda_s)$$

which is assumed to be $\mathcal{O}(1)$. We look for solutions with the expansions

$$V \sim D^{1/2} V_1 + DV_2 + \cdots, \qquad \phi \sim \phi_0 + D^{1/2}\phi_1 + D\phi_2 + \cdots,$$
$$u \sim u_0 + D^{1/2} u_1 + Du_2 + \cdots \quad \text{as } D \to 0.$$

At lowest order we again obtain (17), but now $\phi_0$ solves

$$(\phi_0)'' - s_\phi(\phi_0, e_\infty; \lambda_s) = 0. \tag{20}$$

This is just the steady state version of (18), and a unique solution exists because at $\lambda = \lambda_s$, $s$ has wells of equal depths. At next order in the expansion, we obtain the inhomogeneous linear problem

$$\left(\frac{\mathrm{d}^2}{\mathrm{d}x^2} + f_\phi\right)\phi_1 + f_u u_1 = -V_1\phi_0' + \frac{1}{2}\Lambda u_0 p'(\phi_0), \qquad -\frac{1}{2}p'(\phi_0)\phi_1 + u_1 = -\frac{1}{V_1}u_0',$$

where derivatives of $f$ are computed at the unperturbed quantities $\phi_0, u_0, \lambda_s$. Such a problem only has solutions if the right-hand side is orthogonal to solutions of the homogeneous adjoint problem. In our case, it is easy to see that the vector $[\phi_0', u_0']$ is a null vector of the adjoint operator. We obtain a solvability condition

$$-V_1 I + \Lambda J - \frac{\lambda_s}{V_1} K = 0, \tag{21}$$

where

$$I = \int_{-\infty}^{\infty} (\phi_0')^2 \, \mathrm{d}x, \qquad K = \int_{-\infty}^{\infty} (u_0')^2 \, \mathrm{d}x$$

and

$$J = \frac{1}{2} \int_{-\infty}^{\infty} u_0 p(\phi_0)' \, \mathrm{d}x = \frac{1}{2}(\Delta^2 - u_{\mathrm{m}}^2),$$

where we have used the fact $\frac{1}{2} p(\phi_0)' = u_0'$. The quadratic equation (21) has two roots

$$V_1^{\pm} = \frac{\Lambda J \pm \sqrt{\Lambda^2 J^2 - 4\lambda_s IK}}{2I} \tag{22}$$

as long as

$$\Lambda \geq \frac{\sqrt{\lambda_s IK}}{J}.$$

This means that the velocity $V_1^+$ corresponding to the stable branch of leading front solutions has the lower bound

$$V_1^+ \geq \sqrt{\frac{\lambda_s K}{4I}}.$$

Provided that $\lambda - \lambda_s = \mathcal{O}(D^{1/2})$, the velocity will satisfy

$$V = D^{1/2} V_1 + \mathcal{O}(D), \tag{23}$$

completing our asymptotic analysis.

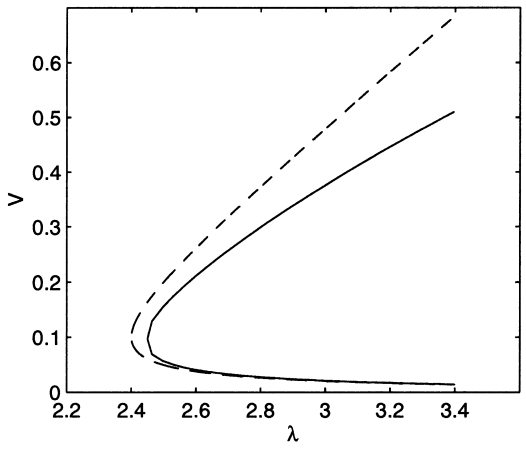


Fig. 5. Approximate velocities obtained from the solvability condition (dashed) and the exact velocities (solid) obtained by numerical solution. The parameters were $D = 0.01$ and $\Delta = 0.5$.

### 4.3. Comparison of the velocities

We now discuss the results of the previous analysis. Eqs. (15), (19) and (23) indicate that, at least when $D$ is sufficiently small, the oscillatory front must be slower than the leading front. Note that when $D = \mathcal{O}(1)$, there is no prediction that the oscillatory front will become faster since the asymptotic expansions may be invalid.

The analysis also provides a tractable way of obtaining quantitative information about front speeds. In particular, the bifurcation of the leading front velocity was explained by the quadratic form of the solvability condition. This result was compared to numerical computations (see Fig. 5) and has reasonably good agreement.

## 5. Discussion

Up to this point, we have only talked about the mathematical aspects of the dual front phenomenon. In this section, we discuss viewpoints concerning its physical meaning.

One interpretation of the intermediate state is a metastable solid phase, such as those described in models of eutectic systems [29,33] which is destabilized, perhaps quite slowly, by diffusion of a conserved quantity (usually some impurity in the alloy). But although the intermediate state is more entropically favorable than the highly undercooled liquid state, the final result is an even more favorable spatially segregated combination of liquid and solid. Numerical simulations indicate that this combination gradually coarsens, much like Cahn–Hilliard systems [7].

Another viewpoint is to regard $\phi$ as a coarse-grained local average of states as mean-field theory does in statistical mechanics. The intermediate state can then be interpreted as a fine mixture of the two phases (in the language of Fife and Gill [14], this is a "mushy zone") which for a given energy level has entropy greater that the liquid. This mixture does not persist, though, by the following mechanism: large wavelength perturbations in the phase mixture lead to regions of higher solid or liquid content. But since $D \neq 0$, latent heat is carried away fast enough so that regions with greater solid (or liquid) content do not remelt (or refreeze).

Numerical experiments indicate that the steady leading front exists only when the thermal diffusion length $D_u/V$ is comparable to the interface width. This is consistent with the asymptotic scaling given in Section 4 (Case 2), since

$$\frac{D_u}{V} \propto \epsilon^2 \frac{D}{V} = \epsilon^2 \mathcal{O}(D^{1/2}) = \epsilon^2 \mathcal{O}(\epsilon^{-1}) = \mathcal{O}(\epsilon).$$

The dual front phenomenon should therefore occur primarily during rapid phase changes. Some examples of phase field models which describe rapid solidification include hypercooled solidification [4] and solute trapping [3]. As in our system, the two field variables in these models vary on comparable scales.

In summary, we have explained why dual front behavior may occur in a generic reaction–diffusion system, and have given conditions for its emergence. Numerical and analytical evidence supports the conclusion that the leading front is always faster, and consequentially the appearance of dual front behavior is governed by the existence of this front.

The question of existence in the traveling wave problem is not as straightforward as it is for single component models, or for their extensions to multicomponent models in which all variables are nonconserved. We remark that numerical evidence suggests that existence becomes more likely for either large undercooling or small diffusion ratio $D$. This is similar to the nonexistence of standard solid–liquid interfaces in the phase field model near unit undercooling [21,22].

## Acknowledgements

This work was supported by the National Science Foundation CAREER program under Award DMS-9502059 and by the NSF MRSEC program under Award DMR-9400379.

## References

[1] R. Almgren, A.S. Almgren, Phase field instabilities and adaptive mesh refinement, in: Long-Qing Chen, B. Fultz, J.W. Cahn, J.R. Manning, J.E. Morral, J. Simons (Eds.), Mathematics of Microstructure Evolution, TMS/SIAM, 1996, pp. 205–214.
[2] D.G. Aronson, H.F. Weinberger, Multidimensional nonlinear diffusions arising in population genetics, Adv. Math. 30 (1978) 33–58.
[3] N.A. Ahmad, A.A. Wheeler, W.J. Boettinger, G.B. McFadden, Solute trapping and solute drag in a phase-field model of rapid solidification, Phys. Rev. E 58 (1998) 3436–3450.
[4] P.W. Bates, P.C. Fife, R.A. Gardner, C.K.R.T. Jones, The existence of travelling wave solutions of a generalized phase-field model, SIAM J. Math. Anal. 28 (1997) 60–93.
[5] J. Bechhoefer, H. Löwen, L.S. Tuckerman, Dynamical mechanism for the formation of metastable phases, Phys. Rev. Lett. 67 (1991) 1266–1269 .
[6] G. Caginalp, Stefan and Hele-Shaw type models as asymptotic limits of the phase-field equations, Phys. Rev. A 39 (1989) 5887–5896.
[7] J.W. Cahn, J.E. Hilliard, Free energy of a nonuniform system. I. Interfacial free energy, J. Chem. Phys. 28 (1957) 258–267.
[8] P. Collet, J.-P. Eckmann, Instabilities and Fronts in Extended Systems. Princeton University Press, Princeton, NJ, 1990.
[9] Z. Csahok, C. Misbah, On the invasion of an unstable structureless state by a stable hexagonal pattern, Europhys. Lett. 47 (1999) 331–337.
[10] G. Dee, J.S. Langer, Propagating pattern selection, Phys. Rev. Lett. 50 (1983) 383–386.
[11] F.J. Elmer, J.-P. Eckmann, G. Hartsleben, Dual fronts propagating into an unstable state, Nonlinearity 7 (1994) 1261–1276.
[12] P.C. Fife, J.B. McLeod, The approach of solutions to nonlinear diffusion equations to traveling front solutions, Arch. Rat. Mech. Anal. 65 (1977) 335–361.
[13] P.C. Fife, Dynamics of Internal Layers and Diffusive Interfaces, SIAM, Philadelphia, PA, 1988.
[14] P.C. Fife, G.S. Gill, The phase field description of mushy zones, Physica D 35 (1989) 267–275.
[15] G. Fix, Phase field methods for free boundary problems, in: A. Fasano, M. Primicerio (Eds.), Free Boundary Problems: Theory and Applications, Vol. 1, Pitman Advanced Publishing Program, 1983, pp. 580–589.
[16] K. Glasner, Traveling waves in rapid solidification, Elec. J. Diff. Eq. 16 (2000) 1–33.
[17] B.I. Halperin, P.C. Hohenberg, Shang-Keng Ma, Renormalization-group methods for critical dynamics. I. Recursion relations and effects of energy conservation, Phys. Rev. B 10 (1974) 139–153.
[18] A.N. Kolmogorov, I.G. Petrovskii, N.S. Piskunov, Study of the diffusion equation with growth of the quantity of matter and its application to a biology problem, in: Selected Works of A.N. Kolmogorov, Kluwer Academic Publishers, Amsterdam, 1991.
[19] A. Karma, W.-J. Rappel, Phase-field method for computationally efficient modeling of solidification with arbitrary interface kinetics, Phys. Rev. E 53 (1996) R3017–R3020.
[20] J.S. Langer, Models of pattern formation in first-order phase transitions, in: G. Grinstein, G. Mazenko (Eds.), Directions in Condensed Matter Physics, Vol. 1, World Scientific, Singapore, 1986.
[21] H. Löwen, J. Bechhoefer, Critical behavior of crystal growth velocity, Europhys. Lett. 16 (1991) 195–200.
[22] H. Löwen, J. Bechhoefer, L.S. Tuckerman, Crystal growth at long times: critical behavior at the crossover from diffusion to kinetics-limited regimes, Phys. Rev. A 45 (1992) 2399–2415.
[23] O. Penrose, P.C. Fife, Thermodynamically consistent models of phase-field type for the kinetics of phase transitions, Physica D 43 (1990) 44–62.
[24] L.M. Pismen, A.A. Nepomnyashchy, Propagation of the hexagonal pattern, Europhys. Lett. 27 (1994) 433.
[25] J. Rubinstein, P. Sternberg, J.B. Keller, Fast reaction, slow diffusion, and curve shortening, SIAM J. Appl. Math. 49 (1989) 116–133.
[26] H.M. Soner, Convergence of the phase-field equations to the Mullins–Sekerka problem with kinetic undercooling, Arch. Rat. Mech. Anal. 131 (1995) 139–197.
[27] L.S. Tuckerman, J. Bechhoefer, Dynamical mechanism for the formation of metastable phases: the case of two nonconserved order parameters, Phys. Rev. A 46 (1992) 3178–3192.
[28] J.E. Taylor, J.W. Cahn, Linking anisotropic sharp and diffuse surface motion laws via gradient flows, J. Stat. Phys. 77 (1994) 183–197.
[29] J. Tiaden, B. Nestler, H.J. Diepers, I. Steinbach, The multiphase-field model with an integrated concept for modelling solute diffusion, Physica D 115 (1998) 73–86.
[30] W. van Saarloos, Dynamical velocity selection: marginal stability, Phys. Rev. Lett. 58 (1987) 2571–2574.
[31] W. van Saarloos, Front propagation into unstable states: marginal stability as a dynamical mechanism for velocity selection, Phys. Rev. A 37 (1988) 211–299.
[32] S.-L. Wang, R.F. Sekerka, A.A. Wheeler, B.T. Murray, S.R. Coriell, R.J. Braun, G.B. McFadden, Thermodynamically-consistent phase-field models for solidification, Physica D 69 (1993) 189–200.
[33] A. Wheeler, W. Boettinger, G. McFadden, Phase-field model for solidification of a eutectic alloy, Proc. Roy. Soc. A 452 (1996) 495–505.
[34] M. Zukerman, R. Kupferman, O. Shochet, E. Ben-Jacob, Concentric decomposition during rapid compact growth, Physica D 90 (1996) 293–305.